ELSEVIER

Physics of the Earth and Planetary Interiors 109 (1998) 107–114

PHYSICS OF THE EARTH AND PLANETARY INTERIORS

Seismic electromagnetic signals (SEMS) explained by a simulation experiment using electromagnetic waves

Qinghua Huang *, Motoji Ikeya

Department of Earth and Space Sciences, Graduate School of Science, Osaka University, Osaka 560-0043, Japan

Received 30 September 1997; revised 4 September 1998; accepted 25 September 1998

Abstract

The propagation characteristics of seismic electromagnetic signals (SEMS) both at an ultra low frequency (ULF) and at a very low frequency (VLF) are discussed based on a model experiment of propagation of electromagnetic (EM) waves in the earth's crust and atmospheric waveguide. A granite slab and two aluminium plates simulated the earth's crust, ionosphere and underground conductive layer, respectively. The Greek archipelago was modeled using a geographical map with the ocean covered by aluminium foil. The intensity of EM waves transmitted from a model hypocenter was mapped to investigate the influence of the ocean. The propagation of VLF waves over the long distance was obtained, while that of ULF indicated the exponential decay from the epicenter. This experiment considered waveguides might explain the ocean's effect on the selectivity and the long distance propagation of SEMS, presumably including seismic electric signals (SES) in the VAN method.

Keywords: Cut-off frequency; Electromagnetic wave; Propagation; Seismic electric signals; Selectivity; Waveguide

1. Introduction

The electromagnetic (EM) phenomena associated with earthquakes are reported in both popular science books and scientific research articles (Varotsos and Alexopoulos, 1984; Oike and Ogawa, 1986; Fujinawa and Takahashi, 1990; Fujinawa et al., 1992, 1997; Wadatsumi, 1995; Electromagnetic Research Group for the 1995 Hyogo-ken Nanbu Earthquake, 1997). Experiments indicated EM emissions can be detected during rock rupture (Nitsan, 1977; Warwick et al., 1982; Ogawa et al., 1985; Cress et al., 1987; Yamada et al., 1989). Some other phenomena correlating with earthquakes, such as lightning and anomalous animal behavior are ascribed to seismic electromagnetic signals (SEMS) (Terada, 1931; Brady and Rowell, 1986; Enomoto and Hashimoto, 1990; Ikeya and Takaki, 1996; Ikeya et al., 1996, 1997). Unfortunately, no consensus is made to explain the long distance propagation of SEMS.

The VAN method of detecting the direct current (DC) voltage in nature as seismic electric signals (SES) claims success in earthquake prediction, especially those of large earthquakes in Greece (Varotsos and Alexopoulos, 1984; Varotsos et al., 1996; Uyeda, 1996). However, the unclear mechanism of SES generation and propagation, as well as the difficulty in distinguishing noise from SES has recently made the VAN method a controversial topic (Lighthill, 1996). What the VAN group detect and whether or not SES can propagate over a long distance from the

* Corresponding author: Fax: +81-6-850-5540; E-mail: chinghua@ess.sci.osaka-u.ac.jp

0031-9201/98/$ - see front matter
PII: S0031-9201(98)00135-6

earthquake epicenters as claimed by the VAN group are main reasons of controversies. Recently, the VAN group presented a hypothesis to explain the possible transmission of SES considering local underground conductivity distribution, which is equivalent to a waveguide of EM waves (Varotsos et al., 1998).

It is not the intention of this paper to question whether the VAN method can predict earthquakes or not. Rather, the topic is the propagation of SEMS both at ultra low frequency (ULF) and at very low frequency (VLF). The characteristics of SEMS propagation in the earth's crust and atmosphere are simulated using a scaling model of the Greek archipelago. The influence of ocean distribution to the selectivity of SEMS is investigated based on a waveguide model experiment of EM waves associated with two earthquakes that occurred in Greece. The SES by the VAN method might be simply due to electric field of EM waves at ULF. Hence, this waveguide experiment might explain the selectivity and the long distance propagation of SES.

2. Experimental

2.1. Waveguide model

We assume that the EM waves could propagate within the following parallel plate waveguides: (1) ionosphere–ocean, (2) ocean–conductive boundary in the crust, and (3) ionosphere–conductive boundary in the crust. A simple theory indicates that the EM waves in a parallel waveguide will satisfy the following relation (Reitz and Milford, 1967, pp. 334–336)

$$1/\lambda_g^2 + 1/\lambda_c^2 = 1/\lambda_0^2, \quad (1)$$

where λ_0 and λ_g are the wavelengths in free space

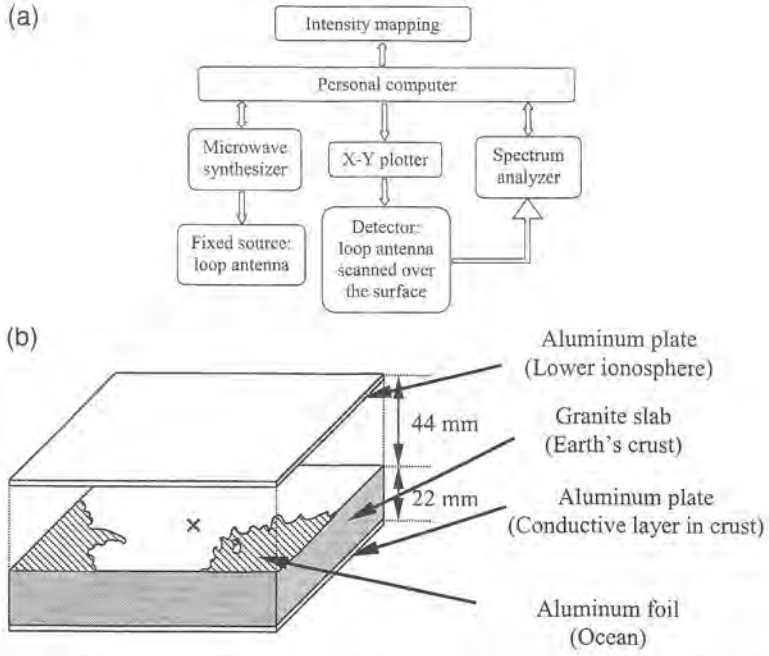

Fig. 1. (a) A schematic diagram of the experimental procedures on the propagation of electromagnetic waves. (b) An experimental model with a granite slab (610 mm × 610 mm × 22 mm) and two aluminium plates simulating the Earth's crust, the lower ionosphere layer and the conductive layer in the crust, respectively. A sketch map of Greek archipelago is drawn on the top surface of the granite slab with the ocean (shadowed part) covered by aluminium foil. Epicenter (marked by a cross) is located at the center of the granite slab.

and in the waveguide, respectively: $\lambda_0 = c/f$ using light speed, c and frequency, f. λ_c is a cut-off wavelength satisfying $\lambda_c = 2a$ for a simple mode using the separation distance between two parallel planes, a.

2.2. Geographic model

The experimental sketch is described in Fig. 1. The Earth's crust (30 km) was simulated by a granite slab (610 mm × 610 mm × 22 mm) with a resistivity of about 10^6 Ω m and a dielectric coefficient, $\varepsilon = 8\varepsilon_0$, where ε_0 is the dielectric coefficient in vacuum. An aluminium plate simulating the conductive boundary in the crust (for simplicity, the Moho plane was assumed in this experiment) was placed against the lower surface of the granite slab. Another aluminium plate at 44 mm above the upper surface of the granite slab simulated the lower ionosphere at 60 km above the ground surface as shown in Fig. 1(b). Although the conductivity of the both planes are different from that of aluminium foil, the overall electric field on the ground surface of our interest, i.e., on the surface of the granite slab in our experiment, is not affected. The Greek archipelago was modeled in a scale of 1:1,360,000 and the conductive sea surface was covered with aluminium foil. The model hypocenter was fixed in a hole at the center from the bottom of the granite slab. The EM signals associated with two earthquakes (M_s (ATH) = 6.6, May 13, 1995; M_s (ATH) = 6.1, June 15, 1995) in Greece were simulated by emission of microwaves from an antenna placed at the model hypocenter. The effect of magnitude cannot be simulated in this simple experiment.

2.3. Electronic systems

A diagram of the experimental procedures including the electronic systems is schematically shown in Fig. 1(a). The source of EM waves is a one-turn loop antenna placed at the hypocenter from a microwave synthesizer (Micro Device, MWSG-18SX) with varied frequency. The detector is another loop antenna close to the surface of the granite slab, which is scanned over the surface by an X–Y plotter (Graphtec, MP 3300) and connected to a spectrum analyzer (Advantest, R 3271). The detected area is 400 mm × 280 mm. The microwave synthesizer, X–Y plotter and spectrum analyzer are all controlled by a personal computer and the data are processed to make a map of EM intensity profile by scanning the detector over the geographical model.

3. Experimental results and discussions

The EM waves at a frequency range from 10^8 Hz to 10^{10} Hz were used to examine the frequency dependence of propagation. Such frequencies would correspond to frequencies of 73.5 Hz to 7350 Hz in the real earth considering the scale of the Greek archipelago model. The power intensity of the source is fixed at 15 dBm (0.0316 W).

The cut-off frequency in the ionosphere–crust waveguide without taking the medium property into account leads to $f_{c1} = c/\lambda_{c1} = c/2a = 2.27$ GHz, which corresponds to 1.67 kHz in the real case (in this paper, we note quantities in the real case in brackets after the model quantities, e.g., 2.27 GHz (1.67 kHz), etc.), using light speed, $c = 3 \times 10^8$ m/s and distance between the ionosphere and the Moho plane, $a = 66$ mm (9×10^4 m). However, considering the complicated media in this waveguide, the cut-off frequency should be less than above estimated value. The ionosphere–ocean wave-

Table 1
Dimensions (separation distance of two parallel planes: a) and cut-off frequencies (f_c) of three waveguides

Waveguide	Separation distance (a)	Cut-off frequency[a] (f_c)
Aluminium (Al) plate-Al plate (Ionosphere–crust)[b]	66 mm (90 km)[b]	< 2.27 GHz (1.67 kHz)[b]
Al plate-Al foil (Ionosphere–ocean)	44 mm (60 km)	3.41 GHz (2.5 kHz)
Al foil-Al plate (Ocean–crust)	22 mm (30 km)	2.41 GHz (1.77 kHz)

[a] $f_c = c*/2a$ using the light speed in the medium, $c*$.
[b] The bracket is the description corresponding to the real earth.

guide model gives a cut-off frequency of $f_{c2} = 3.41$ GHz (2.50 kHz). An ocean–crust waveguide model would have a cut-off frequency of $f_{c3} = 2.41$ GHz (1.77 kHz), considering the light speed in the crust. The dimensions and cut-off frequencies of above different waveguides are tabulated in Table 1.

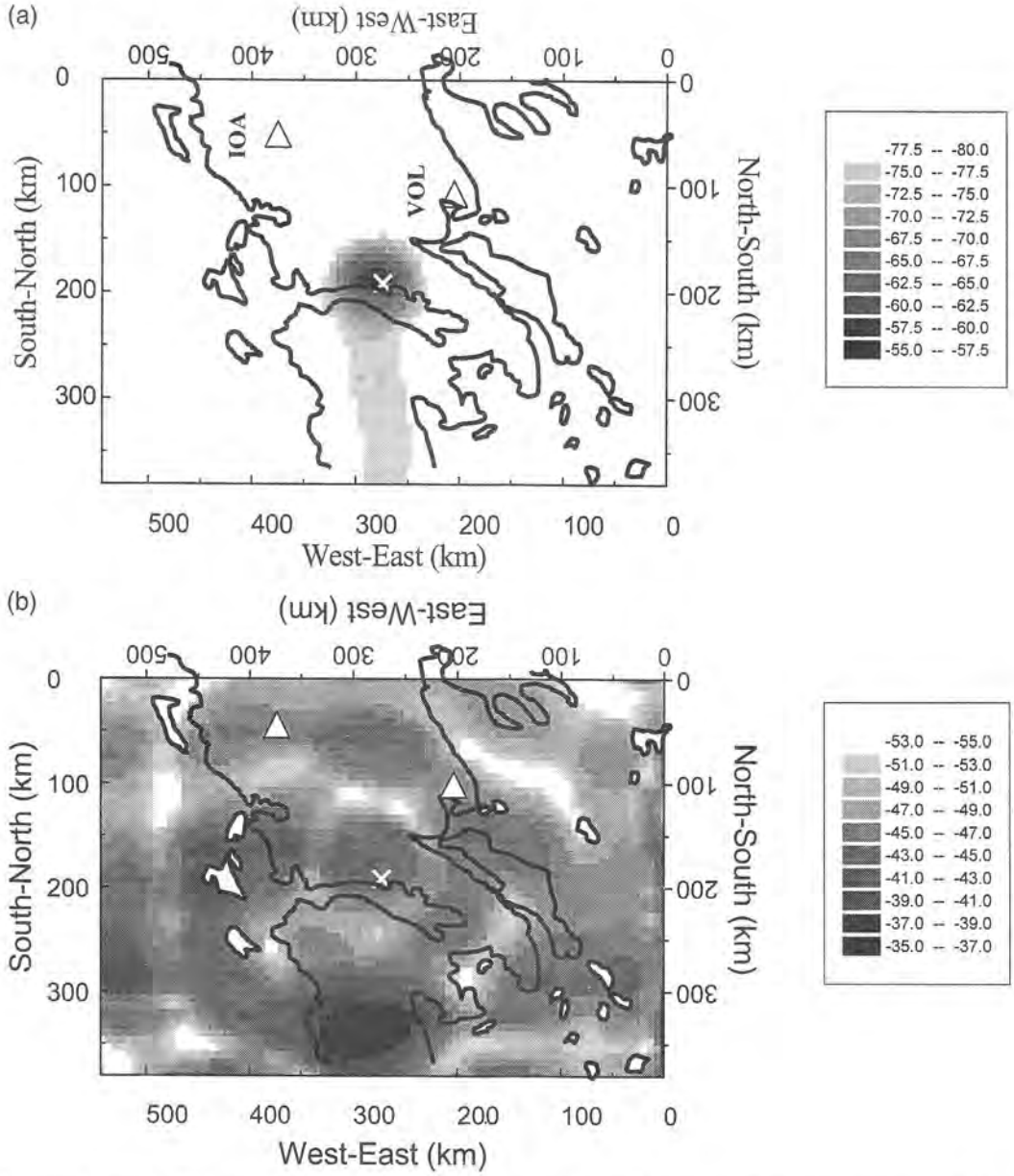

Fig. 2. The intensity map of EM waves on the surface of granite slab without the disturbance of aluminium foil (ocean). The rectangle indicated the scanned region of 544 km × 381 km by the detector, which is 400 mm × 280 mm in our model experiment. The white cross in the center represents the model epicenter and triangles represent VAN's observatories (VOL and IOA). Power intensity is in unit of dBm. (a) Exponential decay at a frequency of 100 MHz (corresponds to 73.5 Hz in the real case). (b) Rippled propagation at a frequency of 2.51 GHz (1.85 kHz).

3.1. Simulation of propagation of EM waves without disturbance of aluminium foil (ocean)

Our experiment simulating the EM wave propagation without aluminium foil (ocean) indicated that the intensity decayed exponentially at a frequency range of 100 MHz (73.5 Hz)–631 MHz (464 Hz). There is an increase in the EM wave intensity with increasing frequency. A rippled propagation was obtained at frequencies ranging from 1 GHz (735 Hz) to 3.98 GHz (2.93 kHz).

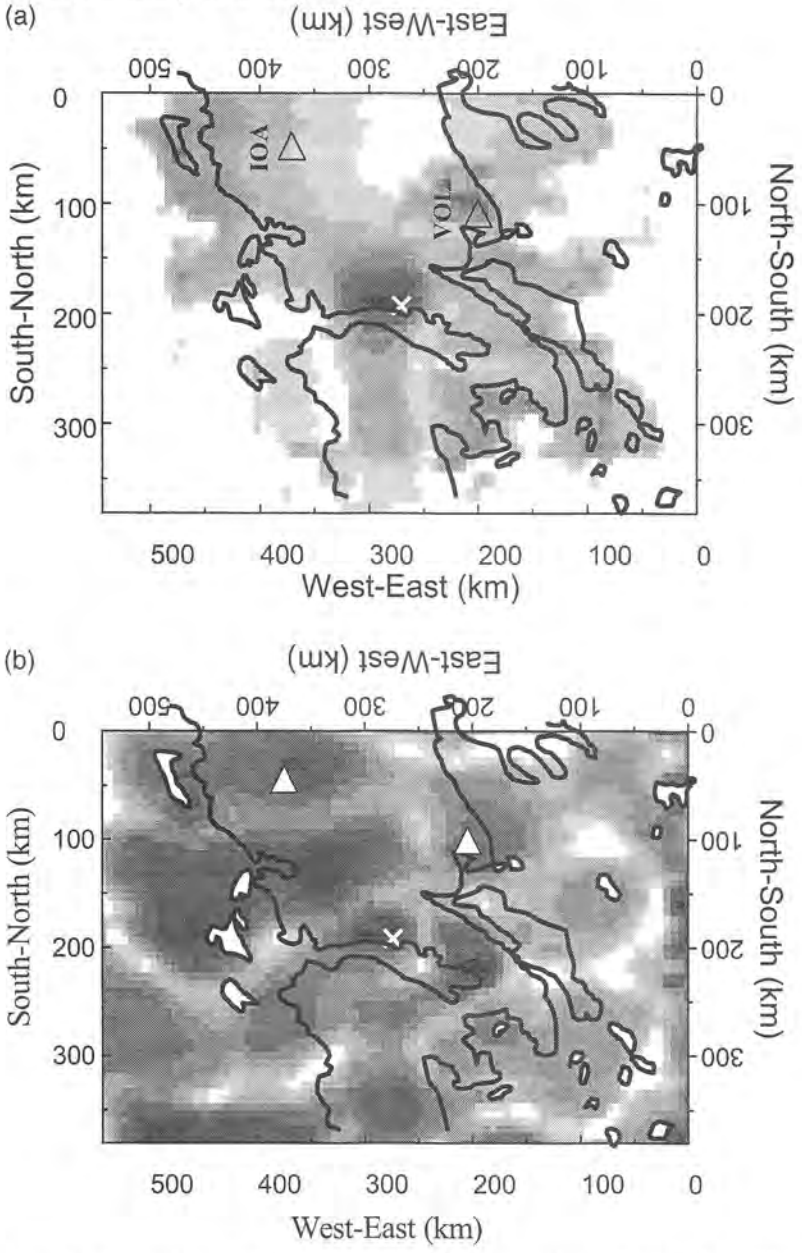

Fig. 3. The intensity map based on the simulation of the propagation of EM waves associated with one M_s (ATH) 6.1 earthquake in Greece. (a) Decay at a frequency of 100 MHz (73.5 Hz) was perturbed by the ocean simulated by aluminium foil. (b) Perturbed rippled pattern at 2.51 GHz (1.85 kHz). (a) and (b) have the same indexes as those in Fig. 2(a) and (b).

Fig. 2(a) indicated that the intensity of EM waves decayed exponentially from the source at a frequency of 100 MHz (73.5 Hz), which is lower than the cut-off frequency, e.g., 2.27 GHz (1.67 kHz). The decay seems to be disturbed by the inhomogeneous grains of the granite slab. Different from the case at a frequency lower than the cut-off frequency, the EM waves can propagate over longer distances at a frequency of 2.51 GHz (1.85 kHz), which is higher than the cut-off frequency. A rippled propagation pattern was observed as shown in Fig. 2(b).

We have investigated the propagation of EM waves associated with one M_s (ATH) 6.6 inland earthquake (May 13, 1995) and one M_s (ATH) 6.1 earthquake (June 15, 1995) with an epicenter close to the Korinthiakos Kolpos bay. Because we keep the model's epicenter at the center of the granite slab and use a fixed source in our experiment, it is the same experiment on the case of no ocean disturbance, no matter if the epicenter is on land or on ocean. The experimental results on the above cases at a low and a high frequency are shown in Fig. 2(a) and (b), respectively.

3.2. Simulation of propagation of EM waves with disturbance of aluminium foil (ocean)

3.2.1. One M_s (ATH) 6.6 earthquake (May 13, 1995)

Similar experiments have been done with the ocean part covered by aluminium foil on the top surface of granite slab (Fig. 1(b)) to investigate the ocean effect on the propagation of EM waves associated with one M_s (ATH) 6.6 earthquake (May 13, 1995). However, we observed similar propagation patterns to those in Fig. 2. The influence of ocean to the propagation of EM waves would not be obvious because the epicenter is located inland rather than in a coastal region.

3.2.2. One M_s (ATH) 6.1 earthquake (June 15, 1995)

The M_s (ATH) 6.1 earthquake occurred in Greece close to the Korinthiakos Kolpos bay on June 15, 1995 was chosen as another example to investigate the ocean effect on the propagation of EM waves. Fig. 3(a) is the intensity map at a frequency of 100 MHz (73.5 Hz), lower than the cut-off frequency. A perturbed distribution is obtained in this case in contrast to that for the M_s (ATH) 6.6 inland earthquake in northern Greece. The VOL observatory detected anomalous SES before the main shock but not IOA (Varotsos et al., 1996). This may be due to the ocean reflection and interference effect because the exponential decay of EM wave intensity is perturbed so that SES may propagate over a long distance. However, we do not claim this pattern is the guided wave mode as appeared at a high frequency but claim the reflection and interference effect by the conductive ocean. Relatively intense EM signals were observed around VOL in this model experiment. We do not claim that present experimental result is consistent with VAN's observations since the underground conductivity distribution might also play a role. We only note the effect of the ocean on the propagation of EM waves.

Fig. 3(b) describes the experimental intensity distribution of EM waves at a frequency of 2.51 GHz (1.85 kHz), which is higher than the cut-off frequency. A perturbed rippled pattern of intensity distribution of EM waves was obtained, which is different for a case having a frequency of 100 MHz (73.5 Hz) lower than the cut-off frequency as shown in Fig. 3(a). Here we found that the intensity of EM

Table 2
Simulation results of the propagation of EM waves associated with one M_s (ATH) 6.1 earthquake (June 15, 1995) in Greece at two frequencies with and without the disturbance of aluminium (Al) foil simulating the ocean

Frequency[a]	Ocean effect	Remarks
100 MHz (73.5 Hz)[a] $< f_{c1}$	Without Al foil	Exponential decay
	With Al foil	Perturbed exponential decay; the selectivity due to ocean reflection
2.51 GHz (1.85 kHz) $> f_{c1}$	Without Al foil	Propagation in a rippled pattern over a long distance
	With Al foil	Propagation in a perturbed rippled pattern over a long distance

[a]The cut-off frequency in the ionosphere–crust waveguide was simply estimated as $f_{c1} < 2.27$ GHz (corresponds to 1.67 kHz in the real earth and is written in the bracket).

signals around the VAN's VOL observatory was more intense than other regions, e.g., the ocean region. The present example also indicated a possible propagation of EM waves at VLF over long distances.

The comparison at two frequencies with and without presence of ocean is summarized in Table 2.

The above analysis indicated the different intensity distribution of SEMS around the epicenter region depending on the geography. If the SES in the VAN method is simply due to the electric field of EM waves at ULF, we should do our experiment at a much lower frequency considering the scaling factor, e.g., ULF waves at 0.1 Hz corresponds to 136 kHz in the model. Unfortunately, we were unable to do the experiment at such a low frequency because of the low S/N ratio. Hence, the exponential decay of the intensity at a frequency (e.g., 100 MHz (73.5 Hz)) lower than the cut-off frequency was extended theoretically to that at ULF (e.g., 136 KHz (0.1 Hz)). The decay is essentially the same as λ_g in Eq. (1) is almost equal to $2a$ in both cases, where a is the separation distance of the parallel plate waveguide. Therefore, we may conclude the ocean effect as one candidate explanation for the selectivity and the long distance propagation of SES, in addition to the underground conductivity distribution as claimed by the VAN group (Varotsos et al., 1996, 1998).

4. Conclusions

A waveguide model experiment was made to investigate the ocean effect on the propagation of SEMS, considering the geography of the Greek archipelago with the ocean part covered by aluminium foil. This experiment indicated that EM waves at a frequency lower than the cut-off frequency decayed exponentially from the source and was disturbed by the presence of ocean. The EM waves at VLF higher than the cut-off frequency showed a rippled pattern of propagation and could propagate over a long distance from the epicenter. Such propagation pattern was also disturbed by the presence of the complicated shape of the ocean. The SES in the VAN method might be simply due to the electric field of EM waves at ULF. Our waveguide experiment would be extended theoretically to the case of ULF. Hence, the selectivity and the long distance propagation of SES might be explained by ocean effect.

Acknowledgements

We thank Dr. T. Yamanaka, K. Kinoshita, T. Takaki and H. Matsumoto for the help of the experiment and useful discussions and Prof. Uyeda for sending us the copies of the recent work of the VAN group and discussion on SES and SEMS. The authors also appreciate Dr. R. Mackie and another anonymous referee for their instructive comments on this manuscript. This research was partially supported by the Sasakawa Scientific Research Grant from the Japan Science Society (Number 10-060).

References

Brady, B.T., Rowell, G.A., 1986. Laboratory investigation of the electrodynamics of rock fracture. Nature 321, 488–492.

Cress, G.O., Brady, B.T., Rowell, G.A., 1987. Sources of electromagnetic radiation from fracture of rock samples in the laboratory. Geophys. Res. Lett. 14, 331–334.

Electromagnetic Research Group for the 1995 Hyogo-ken Nanbu Earthquake, 1997. Tectonoelectric signal related with the occurrence of the 1995 Hyogo-ken Nanbu earthquake (M 7.2) and preliminary results of electromagnetic observation around the focal area. J. Phys. Earth 45, 91–104.

Enomoto, Y., Hashimoto, H., 1990. Emission of charged particles from indentation fracture of rocks. Nature 346, 641–643.

Fujinawa, Y., Takahashi, K., 1990. Emission of electromagnetic radiation preceding the Ito seismic swarm of 1989. Nature 347, 376–378.

Fujinawa, Y., Kumagai, T., Takahashi, K., 1992. A study of anomalous underground electric field variations associated with a volcanic eruption. Geophys. Res. Lett. 19, 9–12.

Fujinawa, Y., Takahashi, K., Matsumoto, T., Kawakami, N., 1997. Experiments to locate sources of earthquake-related VLF electromagnetic signals. Proc. Jpn. Acad. 73, 33–38.

Ikeya, M., Takaki, S., 1996. Electromagnetic fault for earthquake lightning. Jpn. J. Appl. Phys. 35, L355–357.

Ikeya, M., Takaki, S., Takashimizu, D., 1996. Electric shocks resulting in seismic animal anomalous behaviors (SAABs). J. Phys. Soc. Jpn. 65, 710–712.

Ikeya, M., Takaki, S., Matsumoto, H., Tani, A., Komatsu, T., 1997. Pulsed charge model of fault behavior producing seismic electric signals (SES). J. Circuits Syst. Comput. 7, 153–164.

Lighthill, S.J. (Ed.), 1996. A Critical Review of VAN: Earthquake Prediction from Seismic Electrical Signals. World Scientific Press, Singapore, 376 pp.

Nitsan, U., 1977. Electromagnetic emission accompanying fracture of quartz-bearing rocks. Geophys. Res. Lett. 4, 333–336.

Ogawa, T., Oike, K., Miura, T., 1985. Electromagnetic radiations from rocks. J. Geophys. Res. 90, 6245–6249.

Oike, K., Ogawa, T., 1986. Electromagnetic radiations from shallow earthquakes observed in the LF range. J. Geomagn. Geoelectr. 38, 1031–1040.

Reitz, J.R., Milford, F.J., 1967. Foundations of Electromagnetic Theory. Addison-Wesley, 435 pp.

Terada, T., 1931. On luminous phenomena accompanying earthquakes. Bull. Earthq. Res. Inst., Tokyo Univ. 9, 225–255.

Uyeda, S., 1996. Introduction to the VAN method of earthquake prediction. In: Lighthill, S.J. (Ed.), A Critical Review of VAN: Earthquake Prediction from Seismic Electrical Signals. World Scientific Press, Singapore, pp. 3–28.

Varatos, P., Alexopoulos, K., 1984. Physical properties of the variations of the electric field of the earth preceding earthquakes. Tectonophysics 110, 73–98.

Varotsos, P., Lazaridou, M., Eftaxias, K., Antonopoulos, G., Makris, J., Kopanas, J., 1996. Short term earthquake prediction in Greece by seismic electric signals. In: Lighthill, S.J. (Ed.), A Critical Review of VAN: Earthquake Prediction from Seismic Electrical Signals, World Scientific Press, Singapore, pp. 29–76.

Varotsos, P., Sarlis, N., Lazaridou, M., Kapiris, P., 1998. Transmission of stress induced electric signals. J. Appl. Phys. 83, 60–70.

Wadatsumi, K., 1995. Statement 1519 of Earthquake Precursors. Tokyo Press, Tokyo, 265 pp. (in Japanese)

Warwick, J.W., Stoker, C., Meyer, J.R., 1982. Radio emission associated with rock fracture: possible application for the Great Chilean Earthquake of May 22, 1960. J. Geophys. Res. 87, 2851–2859.

Yamada, I., Masuda, K., Mizutani, H., 1989. Electromagnetic and acoustic emission associated with rock fracture. Phys. Earth Planet. Inter. 57, 157–168.